Size-Controlled Synthesis of Spherical TiO_2 Nanoparticles: Morphology, Crystallization, and Phase Transition

Mou Pal,[†] J. García Serrano,[‡] P. Santiago,[§] and U. Pal[‡,*]

Posgrado en Ingeniería y Ciencias Aplicadas, UAEM-CIICAP, Av. Universidad 1001, Col. Chamilpa, 62210-Cuernavaca, Morelos, México, Instituto de Física, Universidad Autónoma de Puebla, Apdo. Postal J-48, Puebla, Pue. 72570, Mexico, and Instituto de Física, Universidad Nacional Autónoma de México, Apartado Postal 20-364, 01000 Mexico D.F., Mexico

Received: March 23, 2006; In Final Form: October 12, 2006

Obtaining spherical-shaped semiconductor nanoparticles of uniform size is essential for the fabrication of photonic crystals. We report the synthesis of nanometer-size spherical titania particles with narrow size distribution from glycolated precursors. Through controlled hydrolysis of glycolated precursors, particles of 683 to 50 nm average diameters, with narrow size distribution, could be produced for the first time. Effects of air annealing on the morphology, size shrinkage, and phase transition of the nanoparticles are studied by scanning electron microscopy, X-ray diffraction, Raman spectroscopy, and high-resolution electron microscopy techniques. Probable mechanisms for formation of titania nanoparticles and their size control are discussed.

Introduction

In recent years, application of nanoparticles is getting more generalized covering different fields including optoelectronics,[1] catalysis,[2] medicine,[3] and sensor devices[4,5] among others. Parameters like structure, size, and elemental composition are considered to be highly important beside the quantum size effects in materials of nanometer scale for their promising applications. Depending on the application, some parameters play a more important role than the others. For example, while composition and size or surface area to volume ratio of the nanoparticles are two vital factors for their applications in catalysis, controlling their shape is vital for fabricating photonic crystals. Among the metal oxide nanostructures, TiO_2 has been extensively explored for several technological applications such as catalysis, gas sensing, white pigments for paints and cosmetics, dye-sensitized solar cells, photochemical degradation of organic pollutants,[6,7] and electrodes in lithium batteries.[8] The applications of titania are found to depend strongly on the crystalline structure, morphology, and particle size.[9] Titanium dioxide occurs mainly in three crystalline phases, namely anatase, rutile, and brookite, which differ in their physical properties, such as refractive index, dielectric constant, and chemical and photochemical reactivity. While rutile is the thermodynamically most stable phase, anatase is preferred for dye-sensitized solar cell, due to its larger band gap ($E_g = 3.2$ eV compared to $E_g = 3.0$ eV for rutile).[10]

Though the application of TiO_2 in fabrication of dye-sensitized solar cells has been well-known since past decade,[11,12] recently it has been tested as an efficient material for generating photonic crystals.[13,14] Among the inorganic semiconductors, titania is an ideal candidate for generating photonic crystals due to its low absorption in the visible and near-infrared regions and relatively higher refractive index ($n = 2.4$ for anatase and 2.9 for rutile).[15] Although for solar cell applications synthesis of titania nanoparticles of selective size and structural phase is crucial, synthesis of monodispersed spherical colloids with minimum size variation (5% or less) is essential for the fabrication of photonic crystals.

Several methods have been developed for generating colloidal titania particles. In industry, titania particles are produced by digesting the ilmenite ore with sulfuric acid followed by thermal hydrolysis of titanium(IV) ions in acidic solution and dehydration of the titanium(IV) hydrous oxides. However, the resulting particles are irregular in shape and highly dispersed in size. Spherical colloids of titania with narrow size dispersion could be achieved through controlled hydrolysis and condensation of appropriate precursors.[16] Matijevi'c and co-workers[17] have successfully prepared stable aqueous colloidal dispersion of titania spheres with diameters ranging from 1 to 4 μm through hydrolysis of $TiCl_4$ in the presence of sulfate ions at elevated temperatures. Barringer and Bowen,[18] and Jean and Ring,[19] prepared titania spheres of 300−700 nm in diameter by controlling the hydrolysis of titanium tetraethoxide in dilute alcohol solutions and could reduce the particle diameter further by adding hydroxypropyl cellulose.[20] Very recently, Jiang et al.[21] produced spherical titania particles of 500−200 nm diameters with very little size dispersion through slow hydrolysis of titanium glycolate precursors. However, synthesis of spherical nanometric titania particles with low size dispersion is still a challenge for their applications in photonic crystal development.

In the present work, titania nanoparticles of controlled size and low dispersions are prepared using a modified sol−gel method. The size and morphology of titania particles exhibited strong dependence on the synthesis conditions. By careful control of the the mixing (concentrations) of reactants and the reaction conditions, morphologically identical titania spheres with average particle size from 50 to 683 nm could be prepared with excellent reproducibility. The amorphous spheres of oxygen deficient titania could be converted to stoichiometric TiO_2 crystals of purely anatase and rutile phases by thermal treatment.

* Corresponding author. E-mail: upal@sirio.ifuap.buap.mx, Fax: +52-222-2295611.
[†] UAEM-CIICAP.
[‡] Universidad Autónoma de Puebla.
[§] Universidad Nacional Autónoma de México.

10.1021/jp0618173 CCC: $37.00
Published on Web 12/09/2006

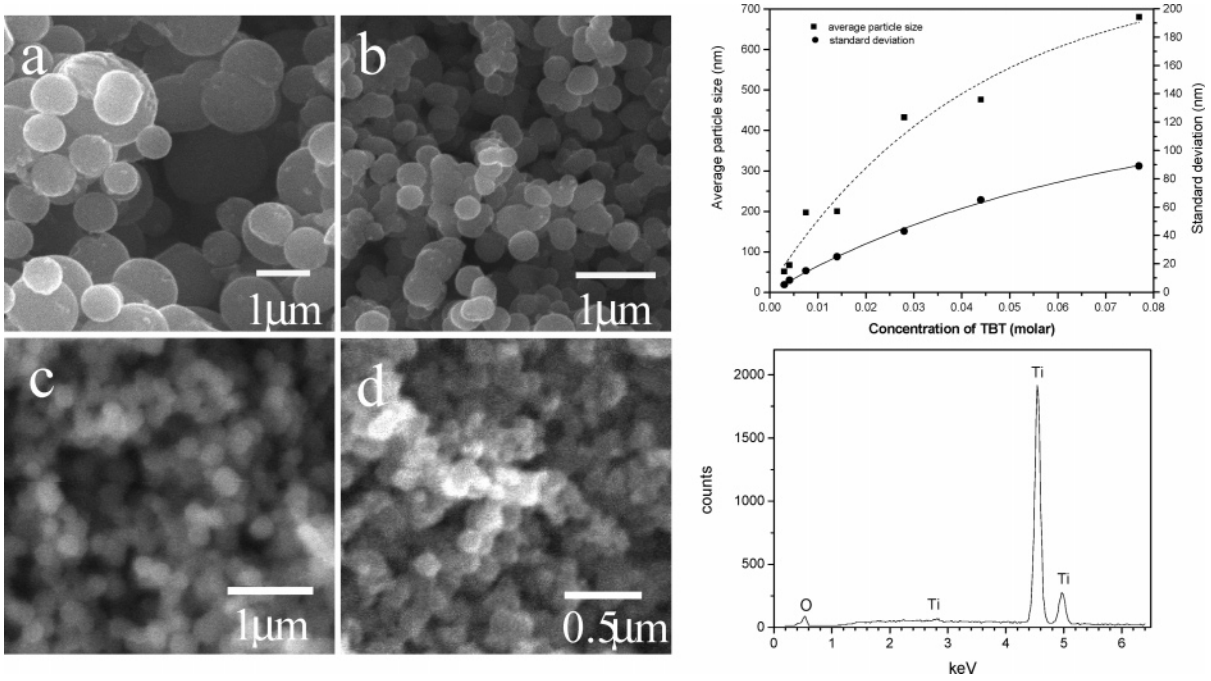

Figure 1. SEM images of titania particles prepared at (a) 0.077, (b) 0.044, (c) 0.007, and (d) 0.004 M TBT in acetone and their average size variation with TBT concentration (right top). The average diameter of the colloids decreased from 683 to 50 nm. The typical EDS spectrum of the particles is shown at the right bottom.

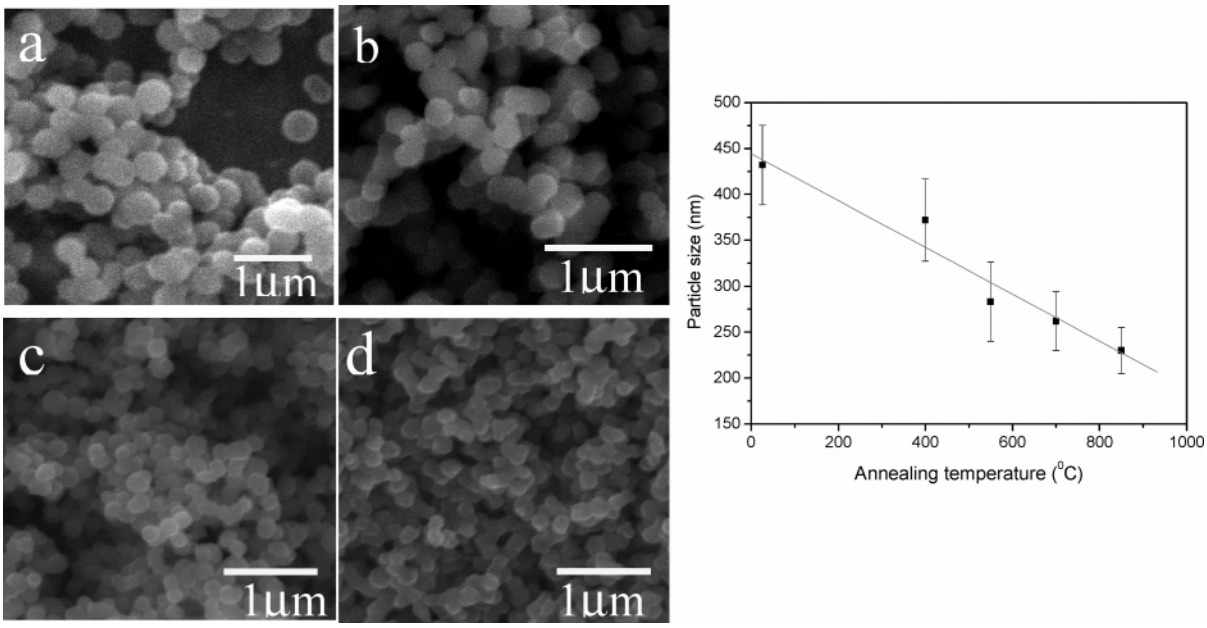

Figure 2. SEM images of titania particles before annealing (a) and after annealing at 550 (b), 700 (c), and 850 °C (d) for 2 h in air and the corresponding size variation (right).

The spherical morphology of the particles was essentially preserved for bigger particles after thermal annealing. Evolutions of morphology, crystallization, and phase transition of the titania particles on air annealing are studied using XRD, SEM, HREM, and Raman spectroscopy techniques.

Experimental Section

Nanometer-size spherical TiO_2 particles were synthesized through the formation of a titanium glycolate intermediate precursor and its controlled hydrolysis. In a typical synthesis, 0.3 mol of tetrabutoxytitanium (TBT, Aldrich 97%) was added to 16 mol of ethylene glycol (Baker) in a glove box under nitrogen atmosphere. The precursor solution was magnetically stirred for 8 h at room temperature and then taken out from the glove box. It is worth mentioning that unlike other titanium alkoxides which are highly susceptible to moisture, the transparent TBT-derived glycolated precursors are more resistant to hydrolysis and could be kept in air for months without forming any precipitate. The glycolated precursor was then poured into acetone (Baker, containing 0.3% water) at different molar concentrations (0.077−0.003 M) under vigorous stirring for about 15−20 min and then kept at rest for 1 h. The transparent precursor solution then became turbid and white, indicating the formation of titania. Though the formation of such white

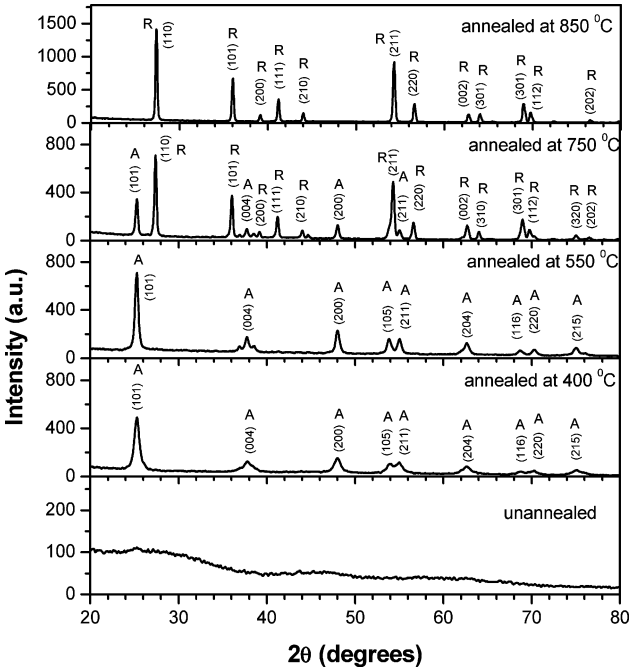

Figure 3. XRD patterns of titania nanoparticles before and after annealing at different temperatures.

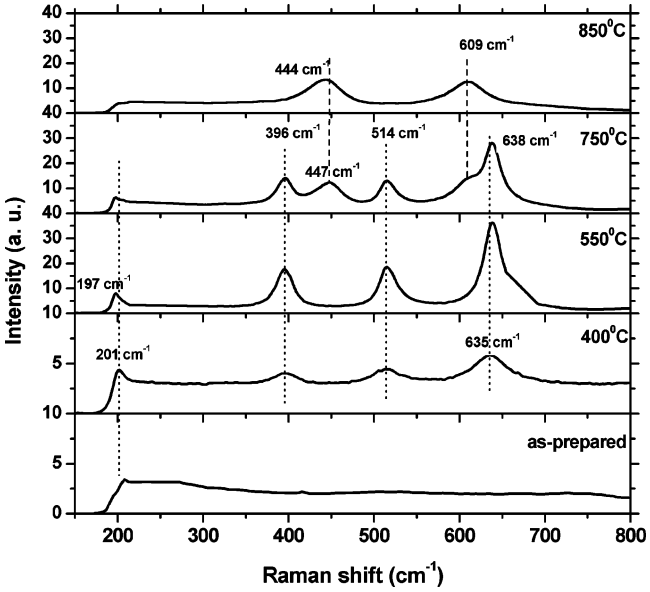

Figure 4. Raman spectra of TiO_2 particles (432 nm average size) annealed at different temperatures.

particles was previously described as titanium glycolate,[21] our chemical analysis results (presented later) clearly demonstrate the formation of nonstoichiometric titania. After the reaction mixture was aged at room temperature for about 1 h, the white precipitate was separated by centrifuging and washed several times with deionized water and ethanol to remove excess ethylene glycol from the surfaces of the particles. Several grams of titania nanoparticles could be produced in this way.

For the hydrolysis of titanium glycolate at different temperatures, the precursor was prepared as stated earlier and hydrolyzed in acetone (0.3% water content) at 2, 15, 35, and 50 °C with a fixed molar concentration (0.0144). The temperature of the reaction mixture during hydrolysis was kept fixed by immersing the reaction flask in ice bath or in warm water bath.

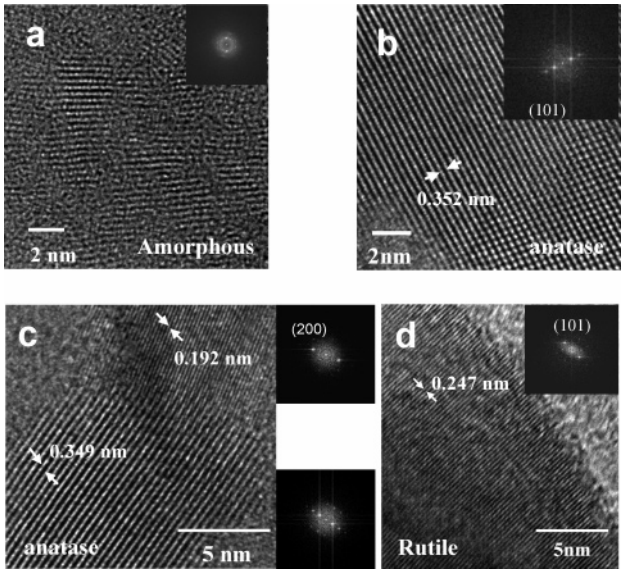

Figure 5. Typical HREM images of titania particles annealed at different temperatures. While the amorphous nature of the as-synthesized particles is clear from the image in part a, the anatase crystalline phase of the particles on annealing at 550 °C is clear in the images in parts b and c. The rutile crystalline phase is clearly depicted in the image of part d. The fast Fourier transforms for the HREM images are shown as insets or beside.

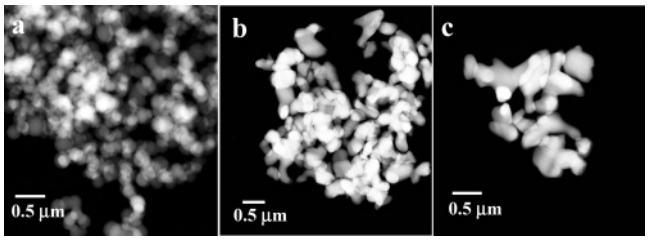

Figure 6. Typical HAADF images of TiO_2 nanoparticles (197 nm average size): (a) unannealed, (b) annealed at 550 °C, and (c) annealed at 850 °C. The particles starts fusing even at 550 °C and form interconnected network structures at higher temperatures.

After drying the samples at room temperature, they were annealed at different temperatures in between 200 and 850 °C in air for 2 h in a horizontal tube furnace. A JEOL JSM 5600LV scanning electron microscope (SEM) with a Noran analytical system attached was used for the morphological and composition analysis of the samples. The monochromatic Cu Kα radiation from a Phillips (X'Pert) diffractometer was used for recording the diffraction traces of the samples. A JEOL FEG 2010 FasTem electron microscope with 1.9 Å resolution (point to point) and high angle annular dark-field detector (HAADF) attached was used for structural characterization of the samples. A Perkin-Elmer NIR Spectrum GX FT-Raman spectrometer with Nd:YAG laser source (1064 nm, 500 mW) was used for recording Raman spectra at room temperature.

Results and Discussion

Spherical colloids of titania were formed through a homogeneous nucleation and growth process. The formation of titanium glycolate precursor can be expressed as:[21]

$$Ti(OBu)_4 + 2\ OHCH_2CH_2OH \rightarrow Ti(OCH_2CH_2O)_2 + 4\ BuOH \quad (1)$$

On adding in acetone, the glycolated precursor undergoes a slow hydrolysis and the spherical titania particles are formed

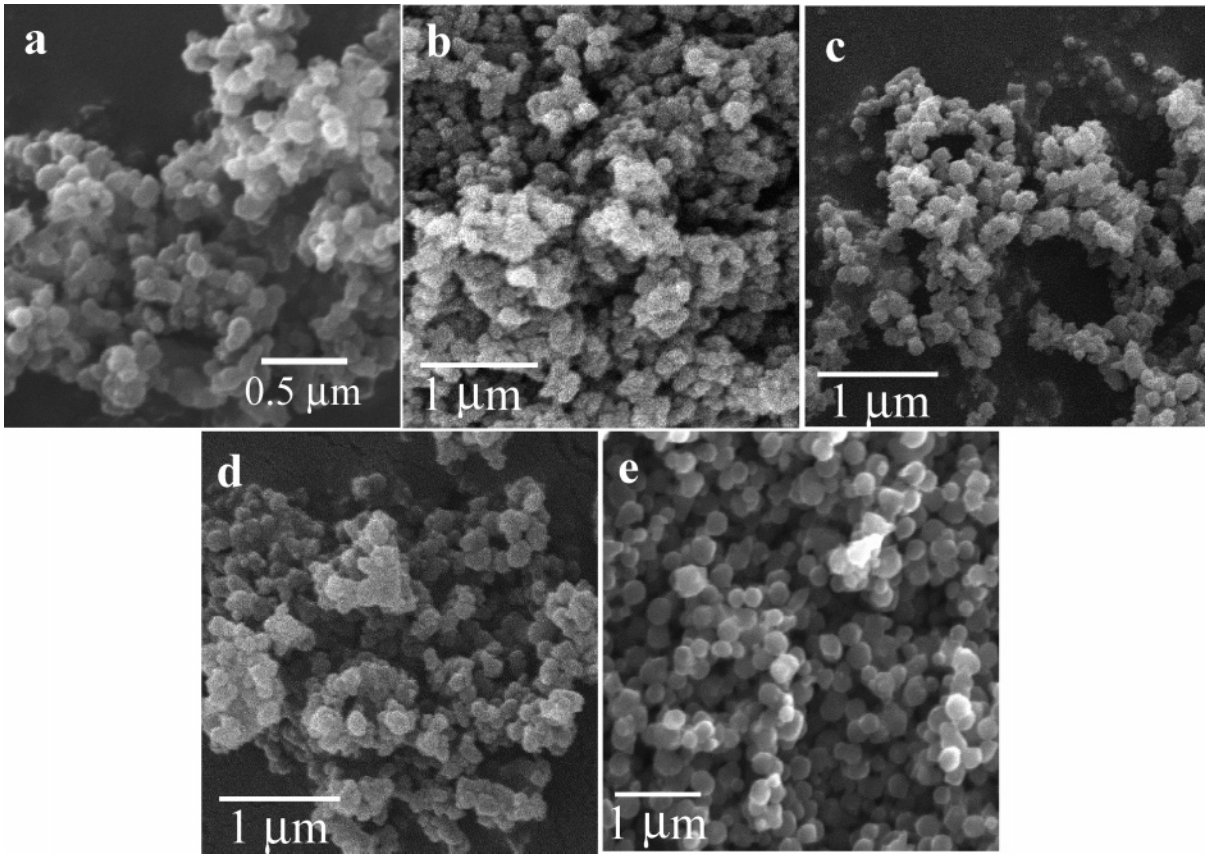

Figure 7. Typical SEM images of TiO_2 particles at different hydrolysis temperature: (a) at 2 °C, (b) at 15 °C, (c) at room temperature (26 °C), (d) at 35 °C, and (e) at 50 °C.

through homogeneous nucleation and growth process. The exact role of acetone is still not very clear, but is believed that it acts as a catalyst to accelerate the hydrolysis rate of the glycolated precursor.[21] However, it is observed tha t the water content in acetone plays an important role on the final size of the particles. While water content more than 0.4% results the formation of inhomogeneous spherical particles, acetone with <0.05% water content does not generate titania particles. We believe, it is water in acetone, which really controls the hydrolysis rate of the glycolated precursor to form titania particles. The hydrolysis process and the formation of titania can be expressed as:

$$Ti(OCH_2CH_2O)_2 + 4H_2O \xrightarrow{\text{hydrolysis}} Ti(OH)_4 + 2\,OHCH_2CH_2OH \quad (2)$$

$$Ti(OH)_4 \xrightarrow{\text{condensation}} TiO_2 \cdot xH_2O + (2 - x)H_2O \quad (3)$$

Transition metal alkoxides are very reactive with moisture, heat, and light due to the presence of highly reactive alkoxide (OR) groups which stabilize metal ions in their highest oxidation states and render them susceptible to nucleophilic attack.[22] In sol−gel processing of metal alkoxides, hydrolysis and condensation reactions occur so rapidly that uniform and fine particles are difficult to obtain. With the use of bulky, branched alkoxy groups such as butoxides, the hydrolysis rates can be reduced as reaction rates decrease with the steric bulk of alkoxy ligands to favor the formation of fine particles with a more uniform size distribution.[23] Another approach to retard the hydrolysis and condensation rates is the chemical modification of metal alkoxides with alcohols, acids or bases, chelating agents, etc. In this work, ethylene glycol was employed as a modifying agent and the modification occurred through nucleophilic substitution reaction (S_N) between the nucleophilic agent ethylene glycol and the metal alkoxide titanium butoxide to produce a molecular precursor, titanium glycolate. As titanium glycolate possesses a symmetric structure which involves bridging occurring through the chelating alkoxy ligend with the ethylene glycol unit, it is more stable to moisture compared to the alkoxide. Another crucial parameter in controlling the hydrolysis reaction rate is the amount of water, defined as the molar ratio with respect to the alkoxide or its glycolate precursor. It has been found that an increase in water content in the hydrolysis reaction produces a higher nucleation rate, resulting in a decrease in average particle size[24−26] and increasing size dispersion.

Figure 1 shows the scanning electron microscope (SEM) images of spherical titania particles prepared at different TBT molar concentrations in acetone. It has been found that primarily TBT concentration in acetone controls the size of the resulting particles. A decrease of the precursor concentration in acetone resulted in a decrease in the average size of titania particles. The average diameter of the particles reduces from 683 to 50 nm by simply changing the precursor concentration from 0.077 to 0.003 M (calculated as the final concentration of the precursor in acetone). While the higher concentration of glycolated precursor in acetone produced particles of dispersed size (Figure 1a), a lower concentration of the precursor produced almost monodispersed (<10% standard deviation) spherical particles. Though the as-synthesized particles were designated as titanium glycolate by Jiang et al.,[21] the appearance of an oxygen peak and the absence of a carbon peak in our energy dispersive X-ray analysis (EDAX) spectra (Figure 1) do not indicate them as titanium glycolate particles. However, the titania particles were not well stoichiometric, with the Ti and O atomic ratio slightly greater than 1:2.

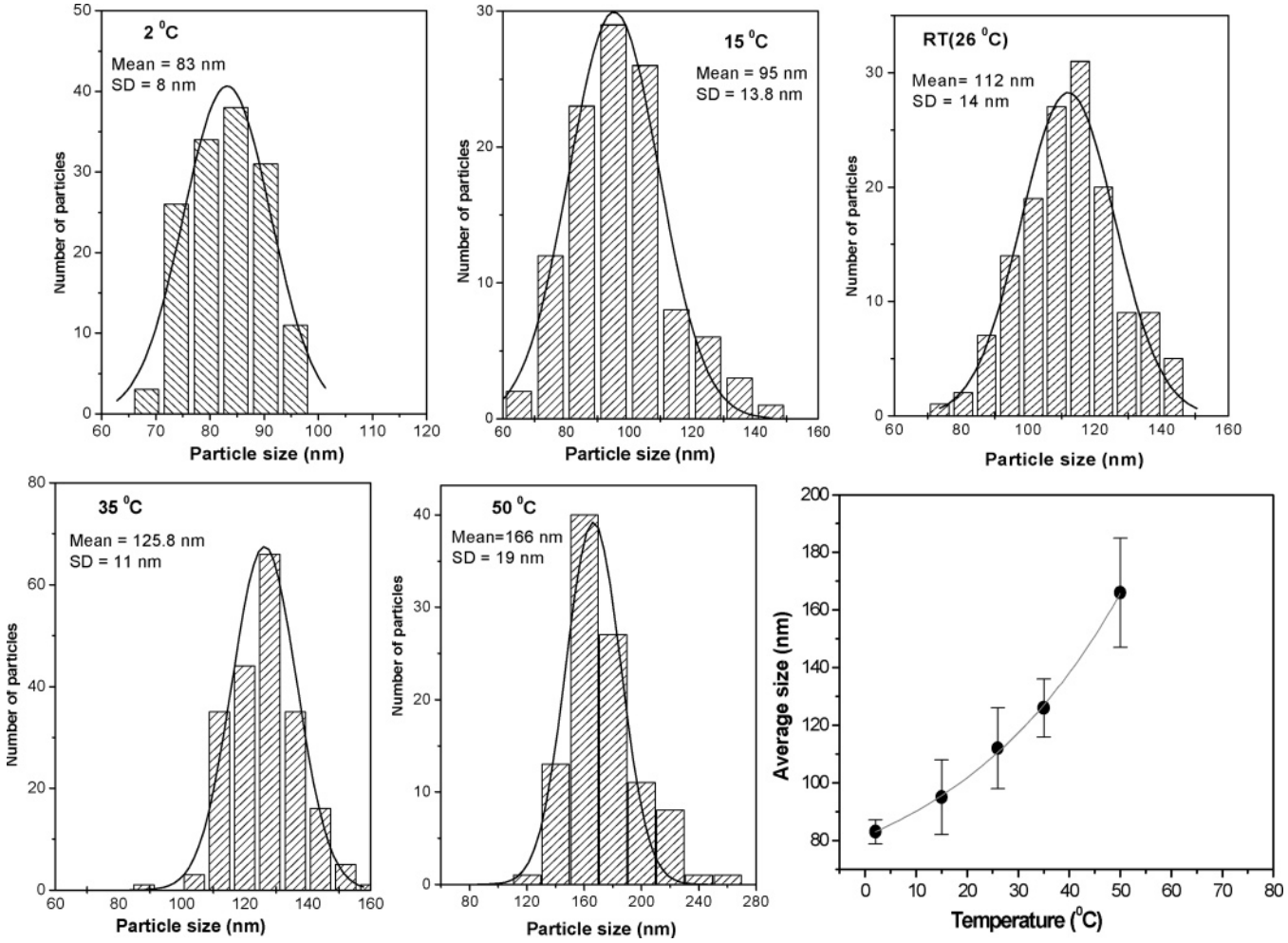

Figure 8. Particle size distribution histograms for the titania particles prepared at different temperatures of hydrolysis. Average particle size and standard deviation are calculated from the Gaussian fittings of the histograms. Variation of particle size (average) with the temperature of hydrolysis is also presented (right bottom). The average size increased exponentially with the temperature of hydrolysis (fitted curve).

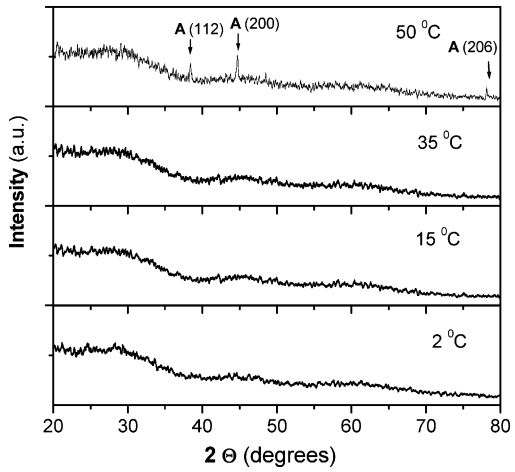

Figure 9. XRD patterns of titania particles prepared at different hydrolyzing temperatures.

In Figure 2, the SEM images of a sample of 432 nm average diameter, before and after annealing at different temperatures in air, are shown. From the images, we can observe that the spherical morphology of the particles is essentially preserved during the annealing process. It is worth noting that the average diameter of the particles is reduced by about 34.5%, 39%, and 46.7% upon annealing the samples at 550, 700, and 850 °C, respectively.

Figure 3 presents the XRD patterns for a sample of 432 nm average particle size before and after annealing. The unannealed sample did not show any diffraction peak, suggesting its amorphous nature. When the sample is annealed at 400 °C, several diffraction peaks appeared and all of them could be clearly attributed to the anatase phase of TiO_2. No other phases such as rutile or brookite could be detected. All the diffraction peaks revealed for the sample annealed at 850 °C correspond to the rutile phase of TiO_2. From XRD patterns, the phase transition from anatase to rutile seemed to occur at 750 °C, as diffraction peaks of both anatase and rutile phases are detected at this temperature. These results are consistent with previously reported results.[27−29]

Annealing induced-phase transitions of TiO_2 particles are further monitored by Raman spectroscopy. Figure 4 shows the Raman spectra of the TiO_2 samples annealed at different temperatures. While the unannealed sample revealed spectral features basically corresponding to the amorphous phase, clearly visible Raman bands appeared at 201, 396, 514, and 635 cm^{-1} for the sample annealed at 400 °C. These bands are the characteristic E_g (low-frequency), B_{1g}, A_{1g} and E_g (high-frequency) vibrational modes of anatase phase,[30,31] respectively. With the increase of annealing temperature to 550 °C, the intensity of these anatase peaks drastically increased along with a red-shift (201 cm^{-1} to 197 cm^{-1}) and a blue-shift (635 cm^{-1} to 638 cm^{-1}) of the E_g (low-frequency) and E_g (high-frequency) modes, respectively. On annealing at 750 °C, along with the

anatase peaks a new peak at 447 cm^{-1} and a shoulder at around 609 cm^{-1} appeared, which correspond to the characteristic E_g and A_{1g} vibrational modes of rutile phase respectively.[32] These two peaks correspond to the bending and stretching modes of TiO_2.[33] For the sample annealed at 850 °C, the intensity of rutile peaks became stronger while the anatase peaks disappeared, indicating a complete phase transition from anatase to rutile in agreement with our XRD results. The 447 cm^{-1} peak broadened and red-shifted (to 443 cm^{-1}). Changes observed in the main Raman peaks of anatase and rutile phases has been interpreted earlier by nonstoichiometry and phonon confinement effects.[34−36] In our case, the as-prepared titania nanoparticles are amorphous and oxygen deficient. Upon annealing in air, the nanoparticles become crystalline, stoichiometric, and of distinct phases depending on the temperature.

In order to study the phase transition in TiO_2 nanoparticles further, we used high-resolution electron microscopy (HREM) technique. In Figure 5, typical HREM images of TiO_2 particles (of about 197 nm average size) annealed at different temperatures in air are presented. While the as-synthesized sample revealed its amorphous nature, crystalline anatase phase is revealed for the sample annealed at 550 °C. On annealing at 850 °C, the anatase phase of the nanoparticles converted fully to rutile phase (Figure 5d). The annealed samples revealed their polycrystalline nature, and the measured interplaner spacings correspond well with the bulk interplaner spacings of corresponding phases.

Further, we observed that the temperatures of phase transitions in TiO_2 nanoparticles and their melting depend strongly on their sizes. The temperatures of phase transition in smaller particles are substantially lower than that of bigger particles. Apart from that, the phase transition process is sharper for smaller particles, and smaller particles start fusing at relatively lower temperatures. For example, we observed that the particles of about 197 nm average size start fusing even at 550 °C (Figure 6), while the particles above 400 nm average size do not fuse even on annealing at 850 °C. In Figure 6, the HAADF images of TiO_2 particles of about 197 nm average size annealed at different temperatures are presented. While the particles start fusing at about 550 °C, they form an interconnected network, completely losing their initial spherical morphology on annealing at 850 °C. Further studies on the effect of particle size on melting and phase transition temperatures in progress.

The size of the spherical titania particles could also be controlled by controlling the hydrolysis temperature of the titanium glycolate precursor. In Figures 7 and 8, typical SEM images of the titania particles prepared at different temperatures of hydrolysis and their size distribution and size variation curves are presented. We can see that the temperature of hydrolysis has a drastic effect on the final size of the titania particles. On increasing the temperature of hydrolysis, the final size of the particles increased exponentially. Therefore, the size of the titania particles could be controlled both by controlling the water content in acetone and by controlling the temperature during hydrolysis. At higher temperature, as the rate of hydrolysis is higher, nanoparticles produced are bigger with high dispersion in size. The titania particles synthesized at low temperatures are amorphous in nature. However, on increasing the temperature of hydrolysis, their crystallinity improves (Figure 9), and for hydrolysis at 50 °C, they start crystallize in the anatase phase. While the titania particles prepared by hydrolyzing titanium glycolate at room temperature are amorphous and a postgrowth thermal annealing (in air) treatment above 350 °C is necessary for their crystallization, hydrolysis of the glycolate precursor at about 50 °C induces crystallization.

It must be noted that while the titanium glycolate precursor could be hydrolyzed in acetone with a controlled water content to produce spherical titania nanoparticles of low dispersion, at such low water contents, they could not be produced using methanol, ethanol, or 2-propanol as hydrolyzing media. As the role of acetone in the hydrolysis process is not yet clear, it needs further investigation to define the role of organic solvents in the hydrolysis.

Conclusion

Spherical TiO_2 nanoparticles of 683 to 50 nm size range and low dispersion could be prepared by controlled hydrolysis of titanium glycolate in acetone. Keeping the water content of acetone to 0.3%, nanoparticles of different sizes could be synthesized either by controlling the concentration of titanium glycolate in acetone or by varying the temperature of hydrolysis. While the higher water content and very high concentration of titanium glycolate in acetone produce titania particles of heterogeneous size, a high temperature of hydrolysis produces bigger particles with higher size dispersion. Synthesized titania particles prepared at room temperature were oxygen deficient and amorphous. The stoichiometry and crystallinity of the particles could be improved by annealing them in air at high temperatures. On air annealing, the titania nanoparticles undergo amorphous−anatase−rutile phase transitions. The phase transitions and melting of titania nanoparticles depend strongly on their sizes. The phase transition and melting temperatures are substantially low for smaller titania particles. To the best of our knowledge, this is the first demonstration of a large scale synthesis of spherical titania particles with low size dispersion and of such a wide range of size. While the titania particles prepared at room temperature are amorphous, and a postgrowth thermal treatment (in air) above 350 °C is must for their crystallization, hydrolysis of the glycolate precursor at about 50 °C induces crystallization. By applying a centrifuge process and air annealing at desired temperatures, monodispersed titania particles of desired size and crystalline phase can be easily prepared for photonic crystals and other applications.

Acknowledgment. We are thankful to E. Aparecio Ceja, CCMC, UNAM, and C. Magaña, IFUNAM for their help in taking XRD traces and SEM images of the samples, respectively. The work was partially supported by the CONACyT, Mexico (Grant No. 46269), and UC-MEXUS-CONACyT (Grant No. CN-05-215).

References and Notes

(1) Tang, Z.; Kotov, N. A.; Giersig, M. *Science* **2002**, *297*, 237.
(2) Campbell, Ch. T.; Parker, S. C.; Starr, D. E. *Science* **2002**, *298*, 811.
(3) Emerich, D. F.; Thanos, C. G. *Exp. Opin. Biol. Ther.* **2003**, *3*, 655.
(4) Pan, Z. W.; Dai, Z. R.; Wang, Z. L. *Science* **2001**, *291*, 1947.
(5) Dong, L. F.; Gui, Z. L.; Zhang, Z. K. *Nanostruct. Mater.* **1997**, *8*, 815.
(6) Zhang, Z.; Wang, C. C.; Zakaria, R.; Ying, Y. J. *J .Phys. Chem. B* **1998**, *102*, 10871.
(7) Dagan, G.; Tomkienviez, M. *J. Phys. Chem. B* **1993**, *97*, 12651.
(8) Kavan, L.; Grätzel, M.; Rathousky, J.; Zukal, A. *J. Electrochem. Soc.* **1996**, *143*, 394.
(9) Wang, W.; Gu, B.; Liang, L.; Hamilton, W. A.; Wesolowski, D. J. *J. Phys. Chem. B* **2004**, *108*, 39.
(10) Kay, A.; Grätzel, M. *Solar Energy Mater. Solar Cells* **1996**, *44*, 99.
(11) O'Reagan, B.; Grätzel, M. *Nature* **1991**, *353*, 737.

(12) Nazeruddin, M. K.; Kay, A.; Podicio, I.; Humphy-baker, R.; Muller, E.; Liska, P.; Vlachopoulos, N.; Grätzel, M. *J. Am. Chem. Soc.* **1993**, *115*, 6382.

(13) Klein, S. M.; Manoharan, V. N.; Pine, D. J.; Lange, F. F. *Langmuir* **2005**, *21*, 6669.

(14) Wijnhoven, J. E. G.; Vos, W. L. *Science* **1998**, *281*, 802.

(15) *Polymer Handbook*, 4th ed.; Brandrup, J., Immergut, E. H., Grulke, E. A., Abe, A., Bloch D. R., Eds.; John Wiley and Sons: New York, 1999; Vol. 93.

(16) Livage, J.; Henry, M.; Sanchez, C. *Prog. Solid State Chem.* **1988**, *18*, 259.

(17) Visca, M.; Matijevic, E. *J. Colloid Interface Sci.* **1979**, *68*, 308.

(18) Barringer, E. A.; Bowen, H. K. *J. Am. Chem. Soc.* **1982**, *65*, C199.

(19) Jean, J. H.; Ring, T. A. *Langmuir* **1986**, *2*, 251.

(20) Jean, J. H.; Ring, T. A. *Colloid Interface Sci.* **1988**, *29*, 273.

(21) Jiang, X.; Herricks, T.; Xia, Y. *Adv. Mater.* **2003**, *15*, 1205.

(22) Brinker C. J.; Scherer, G. W. *Sol-gel Science, The Physics and Chemistry of Sol-Gel Processing*; Academic Press: San Diego, 1990; pp 42−90.

(23) Wang, C-c.; Ying, J. Y. *Chem. Mater.* **1999**, *11*, 3113.

(24) Nagpal, V. J.; Riffe, J. S.; Davis, R. M. *Colloids Surfaces* **1994**, *87*, 26.

(25) Barringer, E. A.; Bowen, H. K. *Langmuir* **1985**, *1*, 414.

(26) Parkar, J. C.; Siegel, R. W. *J. Mater. Res.* **1990**, *5*, 1246.

(27) Tang, J.; Redl, F.; Zhu, Y.; Siegrist, T.; Brus, L. E.; Steigerwald, M. L. *Nano Lett.* **2005**, *5*, 543.

(28) Joint Committee on Powder Diffraction Standard (JCPDS) cards No. 21−1272, and 21−1276.

(29) Cullity, B. D. *Elements of X-Ray Diffraction*; Addison-Wesley: Reading, MA, 1978.

(30) Tompsett, A. G.; Bowmaker, A. G.; Gooney, P. R.; Metson, B. J.; Rodgers, A. K.; Seakins, M. J. *J. Raman Spectrosc.* **1995**, *26*, 57.

(31) Ohsaka, T.; Izumi, F.; Fujiki, Y. *J. Raman Spectrosoc.* **1978**, *7*, 321.

(32) Porto, S. P. S.; Fleury, P. A.; Damen, T. C. *Phys. Rev.* **1967**, *154*, 522.

(33) Traylor, J. G.; Smith, H. G.; Nicklow, R. M.; Wilkinson, M. K. *Phys. Rev. B* **1971**, *3*, 3457.

(34) Parker, J. C.; Siegel, R. W. *J. Mater. Res.* **1990**, *5*, 1246.

(35) Parker, J. C.; Siegel, R. W. *Appl. Phys. Lett.* **1990**, *57*, 943.

(36) Zhang, W. F.; He, Y. L.; Zhang, M. S.; Yiin, Z.; Chen, Q. *J. Phys. D: Appl. Phys.* **2000**, *33*, 912.